Mannose7 Glycan Isomer Characterization by IMS-MS/MS Analysis

Feifei Zhu, **Sunyoung Lee**, **Stephen J. Valentine**, **James P. Reilly**, and **David E. Clemmer**[*]
Department of Chemistry, Indiana University, 800 Kirkwood Ave. Bloomington, IN 47405

Abstract

The isomers of the $Man_7GlcNAc_2$ glycan obtained from bovine ribonuclease B have been characterized by ion mobility spectrometry-tandem mass spectrometry (IMS-MS/MS). In these experiments, $[Man7+2Na]^{2+}$ precursors having different mobilities are selected by ion mobility spectrometry and analyzed by MS/MS techniques in an ion trap. The fragmentation spectra obtained for various precursor ions are specific, suggesting the isolation or enrichment of different glycan isomers. One fragment ion with a mass-to-charge ratio (*m/z*) of 903.8 is found to correspond to the loss of an internal mannose residue of a specific isomer. Extracted fragment ion drift time distributions (XFIDTDs) yield distinctive precursor ion drift time profiles indicating the existence of four separate isomers as proposed previously.

Introduction

In contrast to linear biopolymers such as peptides, proteins and nucleic acids, carbohydrate samples have the potential to be more complex due to multiple linkage sites and stereoisomers of monomer units, the formation of multiple branching patterns, as well as variations in anomeric configurations of glycosidic bonds.[1] Because of this structural diversity, carbohydrates play important roles in biological processes such as cell-cell recognition,[2] immune response,[3] protein regulation,[4] and intercellular signaling.[5,6] To better understand the roles of carbohydrates in such processes, a range of analytical methods have been developed for molecular characterization.[7] However, despite significant progress, characterization of isomer structure is challenging.

In recent years, mass spectrometry (MS) has emerged as a powerful tool for characterizing macromolecular structures. [8–12] Collision-induced dissociation (CID) with MS analysis has been used to identify carbohydrate and glycan sequences as well as glycosylation sites.[13,14] Recently, multi-stage CID (MS^n) experiments have become attractive for sequencing glycans based on comparison to an ion fragment library with algorithms for defining glycan topology. [15–17] However, this method requires a robust fragmentation database and an understanding of the fragmentation mechanisms to select appropriate ions for each dissociation step. The presence of glycan isomers compounds problems associated with this type of analysis. Therefore, experiments have been devised to include condensed-phase separation steps prior to MS analysis in order to identify glycan isomers.[10]

Ion mobility spectrometry (IMS) techniques have recently been coupled to MS analysis to characterize glycans. [18–21] Collision cross section distributions of glycan ions have been interpreted with the aid of molecular modeling techniques to distinguish gas-phase conformations and structural isomers.[18] Additionally, IMS-MS analysis of human serum glycans associated with liver cancer and cirrhosis revealed that IMS distributions of glycans

[*]To whom correspondence should be addressed. clemmer@indiana.edu.

could be used to distinguish phenotypes.[20,21] More recently, a new instrument combining a drift tube with a linear ion trap has allowed MS[n] analysis of mobility-selected carbohydrate species. [22,23] The instrument has been used to characterize a number of isomer mixtures including those containing oligosaccharides, small molecules from a diesel extract, as well as phosphorylated peptides.[22] By monitoring the intensities of fragments unique to isomers across all drift times, extracted fragment ion drift time distributions (XFIDTDs) can be generated corresponding to the mobility distributions of precursor ions. This allows the differentiation of isomers within a mixture having similar drift times.

In this work, the glycans from Ribonuclease B (RNase B) are used as a model system for the IMS-CID-MS analysis. RNase B is a high-mannose glycosylated protein with a single glycosylation site at Asn-34. Isomeric structures of glycans from Ribonuclease B have been characterized by sequential exoglycosidase digestion,[24] proton nuclear magnetic resonance (^{1}H NMR), [25] capillary electrophoresis (CE), [26] and MS. [27] During the last three decades, three structural isomers for $Man_7GlcNAc_2$ have been identified.[24,25] Recently Reinhold and coworkers[27] have proposed an additional isomer based on an elegant study employing MS[n] (n ≥ 5) analysis performed in an ion trap. For this work, the precursor ion was sequentially disassembled to obtain unique fragmentation pathways from which specific glycan topologies were determined. In our study, unique fragments observed for mobility-selected mannose7 glycan ions are used to generate XFIDTDs for distinguishing drift time distributions of different glycan isomers. Comparisons of XFIDTDs show four unique patterns, indicating the presence of four isomeric species for mannose7 glycans, supporting the findings of Reinhold and coworkers.

Experimental

General

IMS theory and instrument design have been previously reported.[28–35] In this work, the IMS-MS analysis was performed on a newly-developed instrument shown in Figure 1. The details regarding different instrumentation components and modes of operation have been reported elsewhere.[22,23] Briefly, the instrument is comprised of a standard electrospray source and desolvation chamber housing an hourglass ion funnel (F1),[36] the drift tube, and a linear ion trap mass spectrometer. The drift tube is ~1 meter long and filled with a buffer gas mixture (~3 torr and 300K) of primarily nitrogen and helium. Electrosprayed ions are accumulated in the back of the F1 region and pulsed into the drift tube at a rate of 55 Hz. As each packet of ions migrates through the drift region, species separate according to the differences in their mobilities through the buffer gas under the influence of a uniform drift field (~2.3×10^3 V/m). Mobility selection of the ions is achieved by applying a gating voltage to the selection gate (Figure 1) at appropriate delay times from the initial ion pulse. A second ion funnel (F2 in Figure 1) focuses the diffuse ion cloud to the center axis of the drift interface region. Mobility-selected ions exiting the drift tube are introduced into a LTQ Velos instrument (Thermo Scientific, San Jose, CA, USA). In the linear ion trap, ions are mass selected and dissociated using CID. Mass-selected ions produce CID fragment ions under a resonant RF excitation waveform applied for 10 ms with 30% normalized collision energy and an activation q of 0.25. For CID of mobility and mass-selected ions, 35% normalized collision energy is used to increase the ion signal of fragments. The resulting spectra are processed using algorithms developed in-house to obtain the nested IMS-MS distributions[37] as well as the extracted drift time distributions of individual ions.[22]

Materials

Ribonuclease B from bovine pancreas, peptide N-Glycosidase F (PNGase F), Chloroform, NaOH beads (97% purity), iodomethane, 2-mecaptomethonal and acetonitrile (ACN) were

purchased from Sigma-Aldrich (St. Louis, MO, USA). Water (HPLC grade) was obtained from EMD Chemicals (Darmstadt, Germany). Dimethylformamide (DMF), trifluoroacetic acid (TFA) and formic acid were obtained from Mallinckrodt Baker (Philipsburg, NJ, USA). C18 micro spin columns, activated charcoal micro spin columns, and empty micro spin columns were all purchased from Harvard Apparatus (Holliston, MA, USA).

Sample Preparation

A detailed procedure of glycan release and permethylation has been published elsewhere.[38] Briefly, 100 μl of ribonuclease B solution (1 mg mL^{-1} in 10 mM sodium phosphate and 0.1% 2-mercaptomethonal buffer at pH 7.5) was thermally denatured at 95 °C for 5 min. After the solution was cooled to room temperature, 0.5 μl of PNGase F (500 mU mL^{-1}) was added, followed by incubation overnight at 37 °C. The released glycans were purified using a C18 micro spin column. The protein/glycan mixture was diluted with 100 μl of aqueous solution containing 5% ACN and 0.1% TFA (solution A) and loaded three times onto the micro spin column pre-conditioned with 400 μl of solution B which is comprised of 15% H$_2$O, 85% ACN and 0.1% TFA. The solution was collected and dried using a vacuum centrifugal concentrator (Labconco Corp., Kansas, MO, USA). The dried glycans were reconstituted with 400 μl of solution A and loaded onto the activated charcoal micro spin column that was preconditioned with solution B. The glycans were washed by 400 μl of solution A three times and then eluted with 400 μl of aqueous solution containing 40% ACN and 0.1% TFA. The samples were subsequently dried under vacuum.

Permethylation of glycans was performed using the spin-column method described previously.[38] The empty column was packed with NaOH beads suspended in ACN up to 1 cm from the top of the column. The purified glycans were mixed with 45 μl of methyl iodine, 60 μl of DMF and 2.4 μl of water and the reaction mixture was loaded onto the packed column preconditioned with DMF. The column was incubated for 15 min before contrifugation. After the second addition of 45 μl of methyl iodine, the mixture was reloaded onto the column and incubated for 15 min. The permethylated glycans were extracted with two applications of 50 μl of ACN and dried under vacuum. Finally, the electrospray solution of the glycans (at a final concentration of ~0.1 mg mL^{-1}) was prepared in 49.9:49.9:0.2 (v: v: v) water: ACN: formic acid and 2 mM sodium acetate solution. The solution was electrosprayed into the instrument at a flow rate of 300 nL min^{-1} using a syringe pump (KD Scientific, Holliston, MA, USA). The needle voltage was maintained at ~2000 V relative to the desolvation chamber entrance aperture.

Results and Discussion

Example IMS-MS dataset

A nested IMS-MS distribution of the permethylated glycans from RNase B is shown in Figure 2. Dataset features for high-mannose glycan ions are observed over a drift time range of ~17 to 24 ms. Five [M+2Na]$^{2+}$ glycans having m/z values of 801.5, 903.5, 1006.0, 1107.9, and 1209.9 are observed in the spectrum. These features have been assigned to the glycans Man$_5$GlcNAc$_2$, Man$_6$GlcNAc$_2$, Man$_7$GlcNAc$_2$, Man$_8$GlcNAc$_2$, and Man$_9$GlcNAc$_2$, respectively. The individual drift time distributions for each glycan can be obtained by integrating a narrow range of m/z values centered about each ion. The work presented here focuses on the characterization of isomeric mannose7 structures. That is, experiments are described for [Man7+2Na]$^{2+}$ ions. The inset in Figure 2 shows the drift time distribution of the [Man7+2Na]$^{2+}$ glycan ion. The precursor ion exhibits a broad drift time distribution from ~20.2 to ~21.6 ms with two unresolved features. Two smaller higher-mobility features at ~19.4 and 19.8 ms are also observed.

MS/MS analysis of [Man7+2Na]$^{2+}$ glycan ions

In presenting the results obtained in the study of the precursor ions, it is instructive to consider the nomenclature for the high mannose glycans as shown in Scheme 1. It has been proposed that the mannose7 glycan can exist as multiple isomeric forms, as additional mannose residues link to the core structure (Scheme 1) by occupying different positions with predefined linkages.[24,39] Four distinct isomeric structures for mannose7 have been previously identified as the D_1, D_2, D_3 and $C_{13}D_{13}$ isomers (Scheme 1).[24–27]

Figure 3a shows the fragmentation spectrum of the [Man7+2Na]$^{2+}$ ions obtained without mobility selection. Collisional activation of oligosaccharides produces three types of fragments: 1) glycosidic fragments that result from the cleavage of a single bond between two neighboring sugar residues; 2) cross-ring fragments that involve the cleavage of two bonds within the sugar ring; and 3) rearrangements in which an internal portion of the structure is eliminated. Glycosidic bond dissociation is predominantly observed in low-energy CID; these fragments provide structural information regarding sequence and branching.[40] Cross-ring fragments are observed at higher collision energies and are useful for identifying linkage types on adjacent sugar residues.[40] As shown in Figure 3, major fragments that are observed upon collisional activation of the [Man7+2Na]$^{2+}$ ions can be assigned as those obtained from non-specific cleavages as well as cleavage of specific bonds associated with individual isomers. Non-specific fragments (labeled in Figure 3) are observed for all isomeric structures and result primarily from glycosidic cleavages. For example, fragment ions at $m/z = 866.8$ are produced from the glycosidic cleavage between the two N-acetylglucosamine residues. Because all isomers have the same reducing terminus, the loss of one N-acetylglucosamine residue cannot be used to distinguish individual isomers. Overall, 13 different fragments have been described as non-specific fragments for the mannose7 glycan ions (Figure 3).

Several of the fragment ions produced by CID of the [Man7+2Na]$^{2+}$ glycan ions can only originate from one or two specific isomers. These result from the different linkage types and occupied sites of the mannose residues. For example, fragment ions at $m/z = 851.4$ can be obtained from the D_1 and D_2 isomers as cross ring cleavage products (Figure 3). However, the D_3 and $C_{13}D_{13}$ isomers cannot produce these fragment ions due to the lack of one mannose residue on the 1–3 linked mannose branch (Figure 3). Additionally, both fragment ions at $m/z = 1043.4$ and 1157.4 are unique for the D_2 and D_3 isomers, but not for the D_1 and $C_{13}D_{13}$ isomers because of different numbers of residues in the 1–6 and 1–3 linked mannose branches. Similarly, the peaks observed at $m/z = 649.3$ and 1361.4 correspond to distinctive fragments for both the D_1 and the $C_{13}D_{13}$ isomers. Finally the $C_{13}D_{13}$ isomer has a unique fragment at $m/z = 903.8$ generated from the loss of an internal mannose residue (see discussion below). Overall, 6 different fragment ions have been described as originating from specific (one or two) glycan isomers.

Although the structurally specific fragments indicate the existence of different mannose7 isomers based on the MS/MS analysis, it is impossible to identify all four isomers because most have no fragments with a unique mass. Higher order tandem MS analysis can alleviate the problem, but relatively high signals for the fragment ions are required for sequential MS^n experiments.

IMS-CID-MS analysis

To demonstrate the isomer characterization abilities of the IMS-MS instrument, CID spectra were recorded across the drift time range of 19.2 to 21.6 ms in increments of 200 µs. Three CID spectra at selected drift times of 20.2 ms, 20.6 ms, and 21.0 ms are shown in Figure 4. For the three collection times, the relative intensities of the non-specific fragment ions at $m/$

$z = 866.8$, 896.3, 989.3, 1257.4, 1288.4, 1465.6, and 1483.5 remain almost identical. The fragment ions at $m/z = 851.4$, 903.8, 1043.4 and 1361.4 that are unique for the D_1/D_2, $C_{13}D_{13}$, D_2/D_3, and $D_1/C_{13}D_{13}$ isomers, respectively, exhibit relative intensities that vary with the selected drift time. For example, the relative intensity ratio of the peaks at $m/z = 1043.4$ to 1361.4 increases by ~5 fold between the drift times at 20.2 ms and 20.6 ms. The peak intensity of the fragment ion at $m/z = 903.8$ decreases sharply from 20.2 ms to 20.6 ms and almost disappears at drift times of 21.0 ms.

Reconstructed drift time profiles from the MS/MS fragments

The drift time distribution of $[Man7+2Na]^{2+}$ precursor ions is shown in Figure 5a (the same distribution as Figure 2 inset). A broad mobility distribution (20.2 ms to 21.2 ms) with partially resolved peaks and two small shoulders at shorter drift times (~19.4 and 19.8 ms) are observed. Previously, we have suggested that a single isomer can have multiple features in the mobility distribution due to the presence of different conformations in the gas phase.[20] It is also possible that different isomers overlap in the mobility distribution due to their similar sizes, resulting in a single broad peak. To distinguish as many isomeric structures of mannose7 as possible, XFIDTDs have been generated for this system. The premise behind this analysis is that by extracting ion intensities of unique fragments across the drift time range, the obtained XFIDTDs are representative of the mobility distribution of specific precursor isomer ions. We have recently shown that XFIDTDs help to distinguish species having identical m/z values and even similar drift times within a mixture.[41]

Figure 5b is the XFIDTD obtained from the non-specific product ions at $m/z = 866.8$. A broad, unresolved distribution is observed across a range of 19.2 to 21.6 ms. The distribution is very similar to the drift time distribution of the precursor ions (Figure 5a). As before, the XFIDTDs for other non-specific fragment ions also present similar distributions (data not shown here). In contrast to the XFIDTDs obtained from non-specific fragment ions, the distributions obtained from each of the unique fragments at $m/z = 1361.4$, 851.4, 1043.4, and 903.8 for the $D_1/C_{13}D_{13}$, D_1/D_2, D_2/D_3 and $C_{13}D_{13}$ isomers, respectively, appear to be different (Figures 5c and 5d). For example, the XFIDTD obtained from the fragment ions at $m/z = 1361.4$ (Figure 5c) that are specific for the $D_1/C_{13}D_{13}$ isomers shows a narrower feature with a peak maximum at 20.8 ms. This feature has a drift time that is identical to a peak maximum in the precursor ion distribution. Also observed is a higher mobility shoulder at 20.4 ms that is identical to the peak maximum of another feature in the precursor ion distribution (although in the former case the feature is of much lower intensity). Figure 5d shows the XFIDTD for the unique fragments ($m/z = 851.4$) of the D_1/D_2 isomers. A broad distribution over the 20.2 to 21.2 ms range with a small shoulder at 20.0 ms is observed. As before, the distribution range and peak maximum of the XFIDTDs are similar to the precursor ion distribution, however, there are differences in the relative intensities of the low- and high- mobility features. For fragments that are specific to the D_2/D_3 isomers (Figure 5e), the XFIDTDs are similar to those obtained for the D_1/D_2 isomers but the relative peak intensity at 20.8 ms is decreased. The XFIDTD for the unique fragment associated with the $C_{13}D_{13}$ isomer shows a dominant peak at 20.3 ms with a small shoulder at 19.6 ms. Notably absent from this dataset is the lower mobility feature (20.8ms).

Internal residue loss determined by XFIDTD

Studies of internal residue loss have been previously reported for both native and permethylated oligosaccharide.[42–46] In high mannose glycans, the 1–6 linked branches have a tendency toward internal rearrangement during MS/MS due to their flexible nature.[45] Of note, Kovac and co-workers have investigated the loss of an internal monosaccharide from 1–6 linked trisaccharides and proposed a mechanism for the internal residue loss.[43] Although these limited studies have pointed out that protonated species are required for

internal rearrangement to occur,[44] here this rearrangement is reported for a doubly sodiated and permethylated mannose7 glycan isomer. We note that subsequent MS^3 analyses support this assignment (see below). It is also noted that although the mechanism is reported for protonated species, it does not preclude the possibility of remote triggering of this process by sodium ions. As shown in Figure 3, all isomers for mannose7 contain 1–6 linked trisaccharides; however, only the $C_{13}D_{13}$ isomer does not have a second branch on the middle mannose in the trisaccharides moiety. If additional mannose residues are attached to the middle mannose, only an internal rearrangement that includes the middle mannose would result in the loss of more than one residue. However, such a branching structure increases steric hindrance and consequently is less likely to lose internal residues via rearrangement.[42] Because the $C_{13}D_{13}$ isomer has a moiety of linearly 1–6 linked trisaccharides without any branching at the middle residue, it is the only species that can produce the fragment ion at $m/z = 903.8$ by internal residue loss.

Although the XFIDTDs generally do not reveal specific IMS features as correlating to specific glycan isomers, the observation of four distinct IMS distributions supports the hypothesis that this glycan exists as four separate isomers. That said, the XFIDTDs do show that the $C_{13}D_{13}$ isomer does not form a low-mobility conformer. Additionally this isomer is comprised of primarily the ions with the highest mobilities (e.g. peak shoulder at 19.6 ms in Figure 5a).

There is another possible fragment that can be assigned to the product ions at $m/z = 903.8$. The cross-ring cleavage of N-acetylglucosamine at the reducing end, which is commonly observed by MS/MS, would also result in fragment ions appearing at the same m/z value. Because all isomers have an identical core structure, this cross-ring cleavage would generate a structurally non-specific fragment. If this were the case, the XFIDTD obtained for the fragment ions at $m/z = 903.8$ might be expected to be similar to that of the precursor ions. As shown in Figure 5, the XFIDTD of the fragment ions is found to be very different. For example, there is no low-mobility feature in the XFIDTD of the $m/z = 903.8$ fragment ions. This suggests that the ions at $m/z = 903.8$ are due to a unique fragmentation of the $C_{13}D_{13}$ isomer. Additionally, the MS^3 spectrum (CID of the fragment at $m/z = 903.8$) reveals a peak at $m/z = 1261.6$, which involves the loss of two N-acetylglucosamine residues (data not shown here), indicating the presence of intact N-acetylglucosamine residues. These results reveal that the fragment ions at $m/z = 903.8$ are produced by the loss of one internal mannose residue. That is, the product ion at $m/z = 903.8$ is specific for the $C_{I3}D_{13}$ isomer.

Comparisons of specific isomeric XFIDTDs

It is worthwhile to examine the XFIDTDs shown in Figure 5. First we note that the distribution obtained for the unique fragment for the $C_{13}D_{13}$ isomer (Figure 5f) does not contain any low mobility features as observed for all other XFIDTDs. In comparison, the distribution obtained for the fragment originating from the $D_1/C_{13}D_{13}$ isomers (Figure 5c) results in a low-mobility feature that dominates the spectrum. High-mobility features that would be associated with the $C_{13}D_{13}$ isomer comprise only a very minor portion of the distribution. Thus it can be deduced that the D_1 isomer forms primarily low-mobility structures. When the specific fragment for the D_1/D_2 isomers is used to create the XFIDTD (Figure 5d), a shift is observed to higher mobility species. Thus it can be argued that the D_2 isomer forms primarily a more compact structure compared to the D_1 isomer. Finally, a comparison of the XFIDTDs obtained from specific fragments for the D_1/D_2 and the D_2/D_3 isomers (Figures 5d and 5e, respectively) reveals a small difference for lower mobility species. For example, as a percentage of the base peak, low mobility species (i.e., with drift times ~ 21 ms) are increased for the latter isomer pair resulting effectively in an overall broader distribution. This indicates that the D_3 isomer contributes a significant portion to the low mobility species in the IMS distribution. Although only one XFIDTD originates solely

from a single isomer, the combination of unique distributions obtained from specific fragments can provide evidence for all four isomers and can yield information about conformer types observed for different isomers. Therefore, in this regard, it is noteworthy that the XFIDTD analysis is useful to differentiate the structurally specific fragments from the shared fragments.

The naturally occurring abundance of high mannose glycans in RNase B has been reported using NMR[25], LC-MS[47], and CE[48] techniques. The mannose7 glycan is the fourth most abundant glycan (~4%) of the total glycan species in RNase B, after mannose5 (~57%), mannose6 (~31%) and mannose8 (7%).[47] The majority of the mannose7 glycan exists as isomer forms D_1, D_2, and D_3 that are reported to have approximately equal proportions.[47] To date, the abundance of isomer $C_{13}D_{13}$ in mannose7 has not been reported, however, it might be expected to exist at lower levels than the other three isomers. This is supported by the fact that isomer $C_{13}D_{13}$ was not previously observed by NMR or condensed-phase separation techniques. Although MS possesses high detection sensitivity, one aspect of multistage MS that hinders the quantification of precursor ions is the lack of knowledge of the efficiencies of formation of specific fragment ions. Therefore it is not possible to estimate the relative amounts of precursor ions based on the intensities of fragment ions. In the present experiment it is noted that the unique fragment ion at $m/z = 903.8$ is observed as one of the more intense isomer-specific fragment ions. Considering the suggested low abundance of the isomer $C_{13}D_{13}$, it may be that the internal rearrangement producing the unique fragment ion occurs at a higher efficiency than the fragmentation pathways producing other specific fragments. Additionally, it is possible that the $C_{13}D_{13}$ isomer exists at higher abundances than had been conjectured.

As mentioned above, the $C_{13}D_{13}$ isomer was first discovered by Reinhold and coworkers using a MS[n] experiment in an ion trap.[27] In contrast to the work presented here, the MS[n] technique is powerful in that it directly identifies isomer structures based on their stepwise disassembly. The XFIDTD strategy is an indirect method that reconstructs the drift time profiles of individual isomer ions and this approach cannot provide a definitive identification for most species. Nevertheless, the XFIDTD approach provides complementary information in the form of evidence for multiple isomers. The presence of unique XFIDTD profiles may indicate the existence of separate isomers; yet a further MS[n] analysis is needed to elucidate the exact isomer structure. Therefore the XFIDTD approach may serve a role of informing MS[n] analyses. The XFIDTD analysis offers the advantage in that for an isomer mixture, it may be used to rapidly provide an indication of the degree of sample complexity by distinguishing isomers without the need for a comprehensive fragmentation analysis.

Another important demonstration of the XFIDTD approach is the potential to quantitate isomeric species such as those reported here. Although the abundances of each isomer may not be predicted directly from their fragment intensities, it may be possible to quantify the relative intensities of each isomer using a new technique that employs Gaussian functions to fit the precursor ion drift time distribution.[49] In this case, the Gaussian functions representing distinct ion populations could be obtained from the reconstructed isomer distributions; that is, the peak positions and widths (in drift time) for all Gaussian functions would be obtained from the XFIDTDs. Using these values, the precursor ion distribution would be fit with the Gaussian functions to provide relative isomer abundances. Noting the timescale of the measurement as well as potential sample quantity limitations, such an ability would be superior to any condensed-phase separation approach. It is also noted that improvements in IMS resolving power would significantly enhance this ability to obtain relative quantitation data for isomeric species.

Summary and conclusions

The structural isomers of mannose7 glycans have been analyzed by IMS coupled with MS^n techniques. The drift time distribution of the $[Man7+2Na]^{2+}$ glycan ion is relatively broad exhibiting at least four local maxima that are attributed to different isomers and/or gas-phase conformations. MS/MS analysis of the precursor glycan ion reveals the presence of product ions that are unique to one or pairs of four proposed isomers. The intensities of several of these fragment ions are observed to vary with precursor ion drift times. XFIDTDs, generated by extracting drift time data centered about the m/z values of the fragment ions, yield mobility distributions that are representative of those for the precursor ions.

Comparisons of the XFIDTDs obtained for fragment ions that are unique to a single isomer (or isomer pair) with the entire glycan distribution show differences in the relative amounts of high- and low-mobility species. Additionally, comparisons of XFIDTDs obtained from different fragment ions reveal a dependence on the precursor ion isomer makeup. Overall such comparisons provide evidence for all four proposed isomers of the mannose7 glycan. Additionally, the XFIDTD method is used to reproduce the mobility distribution of the $C_{13}D_{13}$ isomer of the mannose7 glycan from a mixture of four isomers using a single fragment that is unique to this species. These efforts therefore corroborate the assignment of the $C_{13}D_{13}$ isomer by Reinhold and coworkers.[27] Because the XFIDTDs obtained from other specific fragments represent the distributions of combinations of isomers, it is not currently possible to reproduce the IMS distributions for isomers D_1, D_2 and D_3 separately. However, distribution comparisons do provide some information regarding mobilities for features representing specific isomers. This work thus presents the XFIDTD method as an efficient analysis strategy for determining the presence of multiple glycan isomers without requiring any complicated higher-order MS^n analyses.

Acknowledgments

References

1. Dwek RA. Glycobiology: Toward understanding the function of sugars. Chem Rev. 1996; 96:683–720. [PubMed: 11848770]

2. Campbell CT, Yerema KJ. Large-scale approaches for glycobiology. Genome Biol. 2005; 6:236.0–236.7. [PubMed: 16277754]

3. Bertozzi CR, Kiessling LL. Chemical glycobiology. Science. 2001; 291:2357–2364. [PubMed: 11269316]

4. Rudd PM, Elliott T, Cresswell P, Wilson IA, Dwek RA. Glycosylation and the immune system. Science. 2001; 291:2370–2376. [PubMed: 11269318]

5. Varki A. Biological roles of oligosaccharides: all of the theories are correct. Glycobiology. 1993; 3:97–130. [PubMed: 8490246]

6. Helenius A. Intracellular functions of N-linked glycans. Science. 2001; 291:2364–2369. [PubMed: 11269317]

7. Varki, A.; Cummings, RD.; Esko, JD.; Freeze, HH.; Stanley, P.; Bertozzi, CR.; Hart, GW.; Etzler, ME. Essentials of Glycobiology. Cold Spring Harbor; New York: 2009.

8. Harvey DJ. Quantitative aspects of the matrix-assisted laser desorption mass spectrometry of complex oligosaccharides. Rapid Commun Mass Spectrom. 1993; 7:614–619. [PubMed: 8347867]

9. Zaia J. Mass spectrometry of oligosaccharides. Mass Spectrom Rev. 2004; 23:161–227. [PubMed: 14966796]

10. Mechref Y, Novotny MV. Glycomic analysis by capillary electrophoresis-mass spectrometry. Mass Spectrom Rev. 2009; 28:207–222. [PubMed: 18973241]

11. Williams TI, Saggese DA, Toups KL, Frahm JL, An HJ, Li B, Lebrilla CB, Muddiman DC. Investigations with O-linked protein glycosylations by matrix-assisted laser desorption/ionization Fourier transform ion cyclotron resonance mass spectrometry. J Mass Spectrom. 2008; 43:1215–1223. [PubMed: 18324610]

12. Tang KQ, Li FM, Shvartsburg AA, Strittmatter EF, Smith RD. Two-dimensional gas-phase separations coupled to mass spectrometry for analysis of complex mixtures. Anal Chem. 2005; 77:6381–88. [PubMed: 16194103]

13. Lewandrowski U, Resemann A, Sickmann A. Laser-induced dissociation/high-energy collision-induced dissociation fragmentation using MALDI-TOF/TOF-MS instrumentation for the analysis of neutral and acidic oligosaccharides. Anal Chem. 2005; 77:3274–3283. [PubMed: 15889919]

14. Zhao J, Liu YH, Reichert P, Pflanz S, Pramanik B. Glycosylation analysis of interleukin-23 receptor: elucidation of glycosylation sites and characterization of attached glycan structures. J Mass Spectrom. 2010; 45:1416–1425. [PubMed: 21053369]

15. Ashline D, Singh S, Hanneman A, Reinhold V. Congruent strategies for carbohydrate sequencing. 1. Mining structural details by MS^n. Anal Chem. 2005; 77:6250–6262. [PubMed: 16194086]

16. Takegawa Y, Deguchi K, Ito S, Yoshioka S, Nakagawa H, Nishimura S. Structural analysis of an N-glycan with "beta 1–4 bisecting branch" from human serum IgG by negative-ion MS^n spectral matching exoglycosidase digestion. Anal Chem. 2005; 77:6062–6068. [PubMed: 16159142]

17. Zhang HL, Singh S, Reinhold VN. Congruent strategies for carbohydrate sequencing. 2. FragLib: An MS^n spectral library. Anal Chem. 2005; 77:6263–6270. [PubMed: 16194087]

18. Plasencia MD, Isailovic D, Merenbloom SI, Mechref Y, Clemmer DE. Resolving and assigning N-linked glycan structural isomers from ovalbumin by IMS-MS. J Am Soc Mass Spectrom. 2008; 19:1706–1715. [PubMed: 18760624]

19. Williams JP, Grabenauer M, Holland RJ, Carpenter CJ, Wormald WR, Giles K, Harvey DJ, Bateman RH, Scrivens JH, Bowers MT. Characterization of simple isomeric oligosaccharides and the rapid separation of glycan mixtures by ion mobility mass spectrometry. Intl J Mass Spectrom. 2010; 298:119–127.

20. Isailovic D, Kurulugama RT, Plasencia MD, Stokes ST, Kyselova Z, Goldman R, Mechref Y, Novotny MV, Clemmer DE. Profiling of human serum glycans associated with liver cancer and cirrhosis by IMS-MS. J Proteome Res. 2008; 7:1109–1117. [PubMed: 18237112]

21. Isailovic D, Plasencia M, Gaye M, Stokes S, Kurulugama R, Pungpapong V, Zhang M, Kyselova Z, Goldman R, Mechref Y, Novotny MV, Clemmer DE. Delineating diseases by IMS-MS profiling of serum N-linked glycans. J Proteome Res. 2012; 11:576–585. [PubMed: 22148953]

22. Zucker SM, Lee S, Webber N, Valentine SJ, Reilly JP, Clemmer DE. An ion mobility/ion trap/photodissociation instrument for characterization of ion structure. J Am Soc Mass Spectrom. 2011; 22:1477–1485. [PubMed: 21953250]

23. Lee S, Valentine SJ, Zucker SM, Webber N, Reilly JP, Clemmer DE. Extracted fragment ion mobility distributions: a new method for complex mixture analysis. Intl J Mass Spectrom. 2012; 309:154–160.

24. Liang C, Yamashita K, Kobata A. Structural study of carbohydrate moiety of bovine pancreatic ribonuclease B. J Biochem. 1980; 88:51–58. [PubMed: 7410340]

25. Fu DT, Chen L, Oneill RA. A detailed structural characterization of ribonuclease B by ^{1}HNMR spectroscopy and mass spectrometry. Carbohydr Res. 1994; 261:173–186. [PubMed: 7954510]

26. Zhuang Z, Starkey JA, Mechref Y, Novotny MV, Jacobson SC. Electrophoretic analysis of N-glycans on microfluidic devices. Anal Chem. 2007; 79:7170–7175. [PubMed: 17685584]

27. Prien JM, Ashline DJ, Lapadula AJ, Zhang H, Reinhold VN. The high mannose glycans from bovine ribonuclease B isomer characterization by ion trap MS. J Am Soc Mass Spectrom. 2009; 20:539–556. [PubMed: 19181540]

28. Revercomb HE, Mason EA. Theory of plasma chromatography/gaseous electrophoresis- a review. Anal Chem. 1975; 47:970–983.

29. Mack E. Average cross-sectional areas of molecules by gaseous diffusion methods. J Am Chem Soc. 1925; 47:2468–2482.

30. Shvartsburg AA, Jarrold MF. An exact hard-spheres scattering model for the mobilities of polyatomic ions. Chem Phys Lett. 1996; 261:86–91.

31. Clemmer DE, Hudgins RR, Jarrold MF. Naked protein conformations: cytochrome c in the gas phase. J Am Chem Soc. 1995; 117:10141–10142.

32. Helden G, von Wyttenbach T, Bowers MT. Conformation of macromolecules in the gas phase: use of matrix-assisted laser desorption methods in ionchromatography. Science. 1995; 267:1483–1485. [PubMed: 17743549]

33. Valentine SJ, Koeniger SL, Clemmer DE. A split-field drift tube for separation and efficient fragmentation of biomolecular ions. Anal Chem. 2003; 75:6202–6208. [PubMed: 14616002]

34. Kanu AB, Dwivedi P, Tam M, Matz L, Hill HH Jr. Ion mobility-mass spectrometry. J Mass Spectrom. 2008; 43:1–22. [PubMed: 18200615]

35. Hoaglund CS, Valentine SJ, Sporleder CR, Reilly JP, Clemmer DE. Three dimensional ion mobility/TOFMS analysis of electrosprayed biomolecules. Anal Chem. 1998; 70:2236–2242. [PubMed: 9624897]

36. Tang K, Shvartsburg AA, Lee HN, Prior DC, Buschbach MA, Li F, Tolmachev AV, Anderson GA, Smith RD. High-sensitivity ion mobility spectrometry/mass spectrometry using electrodynamic ion funnel interfaces. Anal Chem. 2005; 77:3330–3339. [PubMed: 15889926]

37. Hoaglund CS, Valentine SJ, Sporleder CR, Reilly JP, Clemmer DE. Three-dimensional ion mobility/TOFMS analysis of electrosprayed biomolecules. Anal Chem. 1998; 70:2236–2242. [PubMed: 9624897]

38. Kang P, Mechref Y, Klouckova I, Novotny MV. Solid-phase permethylation of glycans for mass spectrometric analysis. Rapid Commun Mass Spectrom. 2005; 19:3421–3428. [PubMed: 16252310]

39. Kurimoto A, Kanie O. Distinguishing isomeric pyridylaminated high-mannose (man$_7$) oligosaccharides based on energy-resolved mass spectra. Rapid Commun Mass Spectrom. 2007; 21:2770–2778. [PubMed: 17659657]

40. Harvey D. Collision-induced fragmentation of underivatized N-linked carbohydrates ionzed by electrospray. J Mass Spectrom. 2000; 35:1178–1190. [PubMed: 11110090]

41. Lee S, Valentine SJ, Reilly JP, Clemmer DE. Analyzing a mixture of disaccharides by IMS-VUVPD-MS. Intl J Mass Spectrom. 2012; 309:161–167.

42. Harvey DJ, Mattu TS, Wormald MR, Royle L, Dwek RA, Rudd AM. "Internal residue loss": rearrangements occurring during the fragmentation of carbohydrates derivatized at the reducing terminus. Anal Chem. 2002; 74:734–740. [PubMed: 11866052]

43. Brüll LP, Heerma W, Thomas-Oates J, Haverkamp J, Kovácik V, Kovác P. Loss of internal 1–6 substituted monosaccharide residues from underivatized and per-o-methylated trisaccharides. J Am Soc Mass Spectrom. 1997; 8:43–49.

44. Brüll LP, Kovácik V, Thomas-Oates JE, Heerma W, Haverkamp J. Sodium-cationized oligosaccharides do not appear to undergo 'internal residue loss' rearrangement processes on tandem mass spectrometry. Rapid Commun Mass Spectrom. 1998; 12:1520–1532. [PubMed: 9796537]

45. Wuhrer M, Koeleman CAM, Deelder AM. Hexose rearrangements upon fragmentation of N-glycopeptides and reductively aminated N-glycans. Anal Chem. 2009; 81:4422–4432. [PubMed: 19419147]

46. Kovácik V, Hirsch J, Kovác P, Heerma W, Thomas-Oates J, Haverkamp J. Oligosaccharide characterization using collision-induced dissociation fast atom bombardment mass spectrometry : evidence for internal monosaccharide residue loss. J Mass Spectrom. 1995; 30:949–958.

47. Costello CE, Contado-Miller JM, Cipollo JF. A glycomics platform for the analysis of permethylated oligosaccharide alditols. J Am Soc Mass Spectrom. 2007; 18:1799–1812. [PubMed: 17719235]

48. Guttman A, Pritchett T. Capillary gel electrophoresis separation of high-mannose type oligosaccharides derivatized by 1-aminopyrene-3,6,8-trisulfonic acid. Electrophoresis. 1995; 16:1906–1911. [PubMed: 8586063]

49. Shi H, Pierson NA, Valentine SJ, Clemmer DE. Conformation types of ubiquitin [M+8H]8+ ions from water: methanol solutions: evidence for the N and A states in aqueous solution. J Phys Chem B. 2012; 116:3344–3352. [PubMed: 22315998]
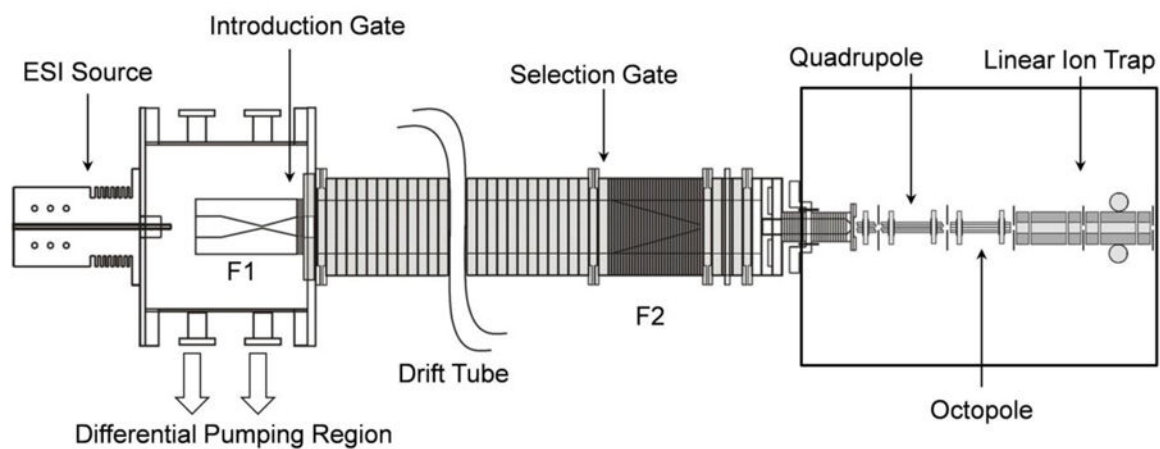
Figure 1.
Schematic diagram of the IMS-MS instrument used in these studies. The instrument is comprised of an ESI source, a drift tube, and a linear ion trap. See the experimental section for additional details.
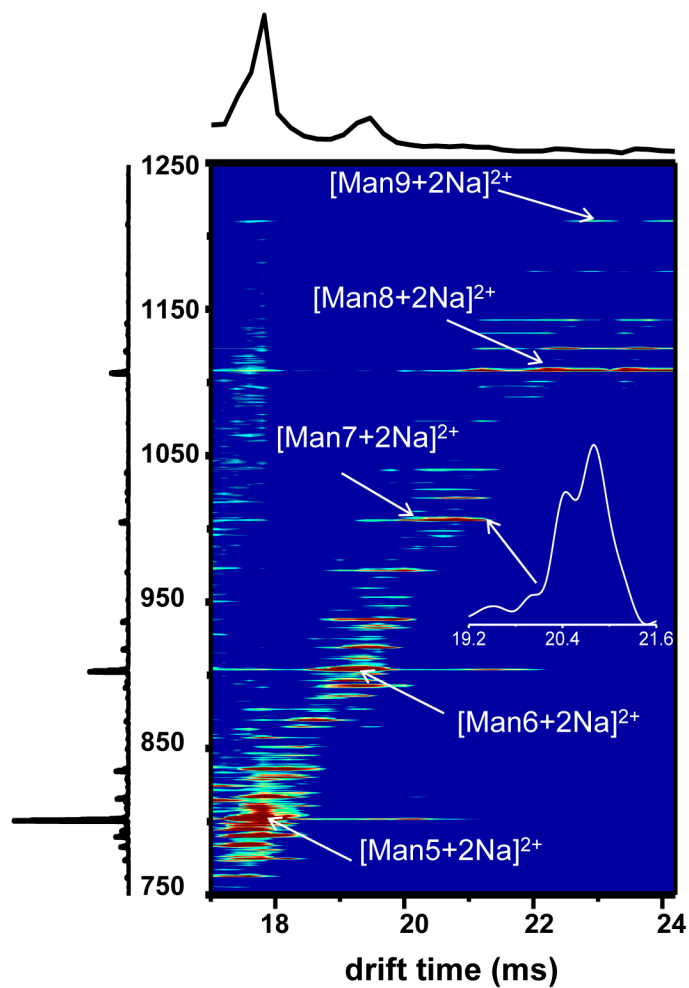
Figure 2.
Nested IMS-MS distribution for the electrosprayed high mannose glycans ions derived from RNase B. Across the top is the total drift time distribution obtained by integrating data points over entire m/z range for each drift bin. Across the left shows the total mass spectrum obtained by integrating data points over entire drift range for each m/z bin. Figure inset displays the drift time distribution of the doubly-sodiated $Man_7GlcNAc_2$ glycan ions, obtained by integration of the drift bins across a narrow m/z range.
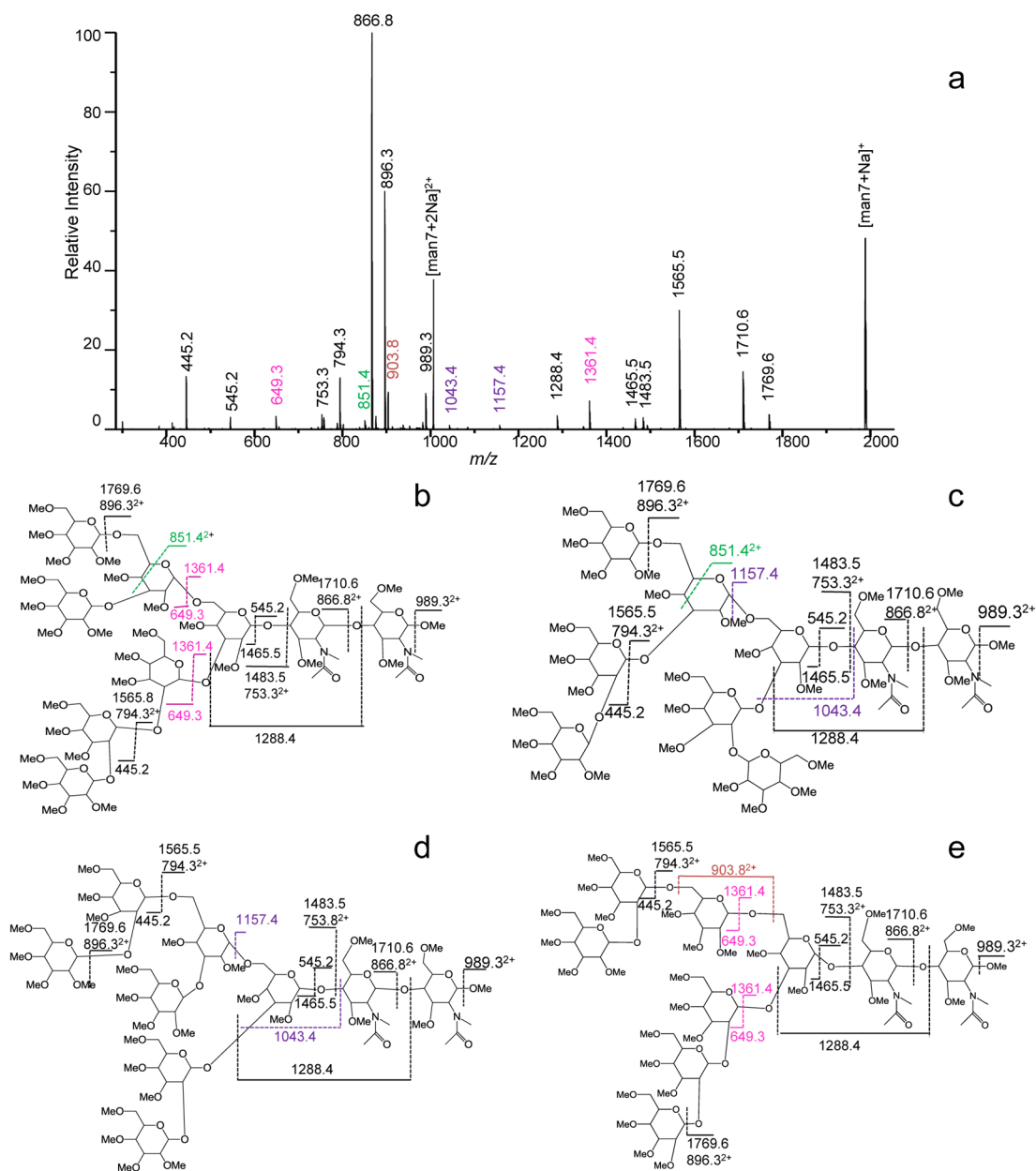
Figure 3.
(a) CID spectrum of the [Man7+2Na]$^{2+}$ glycan precursor ion without mobility selection; schematic representations of the (b) D$_1$, (c) D$_2$, (d) D$_3$, and (e) C$_{13}$D$_{13}$ isomers with CID fragment ions are also presented. Black labels represent non-specific fragments. Pink, purple, green, and brown labeled fragments can be specifically generated from the D$_1$/C$_{13}$D$_{13}$, D$_2$/D$_3$, D$_1$/D$_2$, and C$_{13}$D$_{13}$ isomers, respectively.
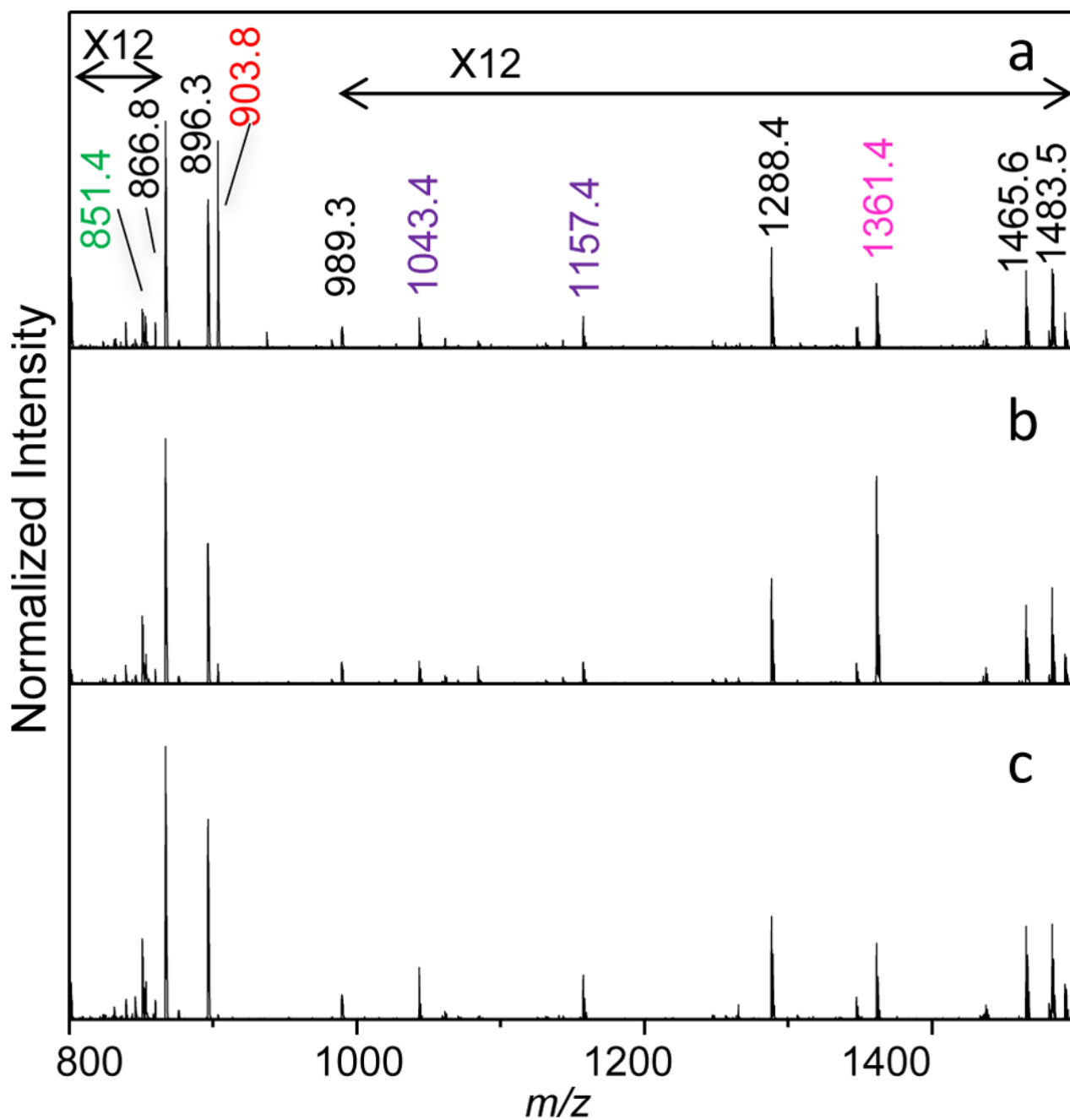
Figure 4.
CID spectra of the mobility-selected ions at (a) 20.2, (b) 20.6, and (c) 21.0 ms. Unique fragments are labeled in colors (Figure 3) and non-specific fragments are shown in black. The m/z range has been narrowed (800 to 1500) for a closer comparison between the spectra.
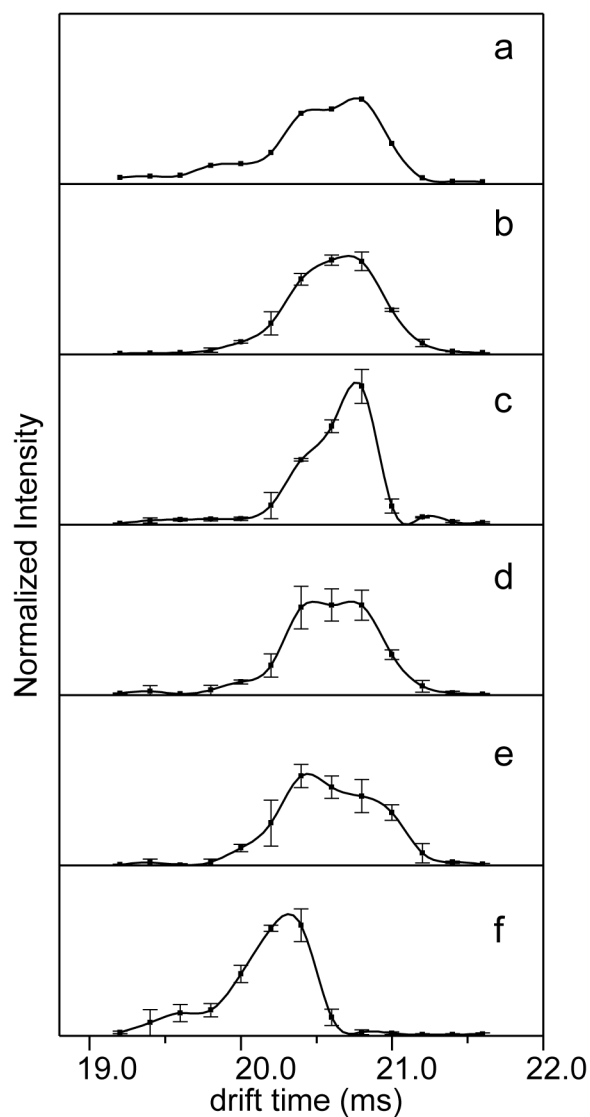
Figure 5.
(a) Ion mobility distribution of the precursor ions ($m/z = 1006.0$). XFIDTDs obtained from (b) the non-specific fragment ions ($m/z = 866.8$) and the specific fragments at m/z (c) 1361.4, (d) 851.4, (e) 1043.4, and (f) 903.8 for the $D_1/C_{13}D_{13}$, D_1/D_2, D_2/D_3 and $C_{13}D_{13}$ isomers, respectively. The distributions represent the averages of three data sets with the error bars representing the standard deviation at each drift time. These distributions are observed by integrating all drift bins over a narrow range (centered about the m/z values given above) for each drift time selection.
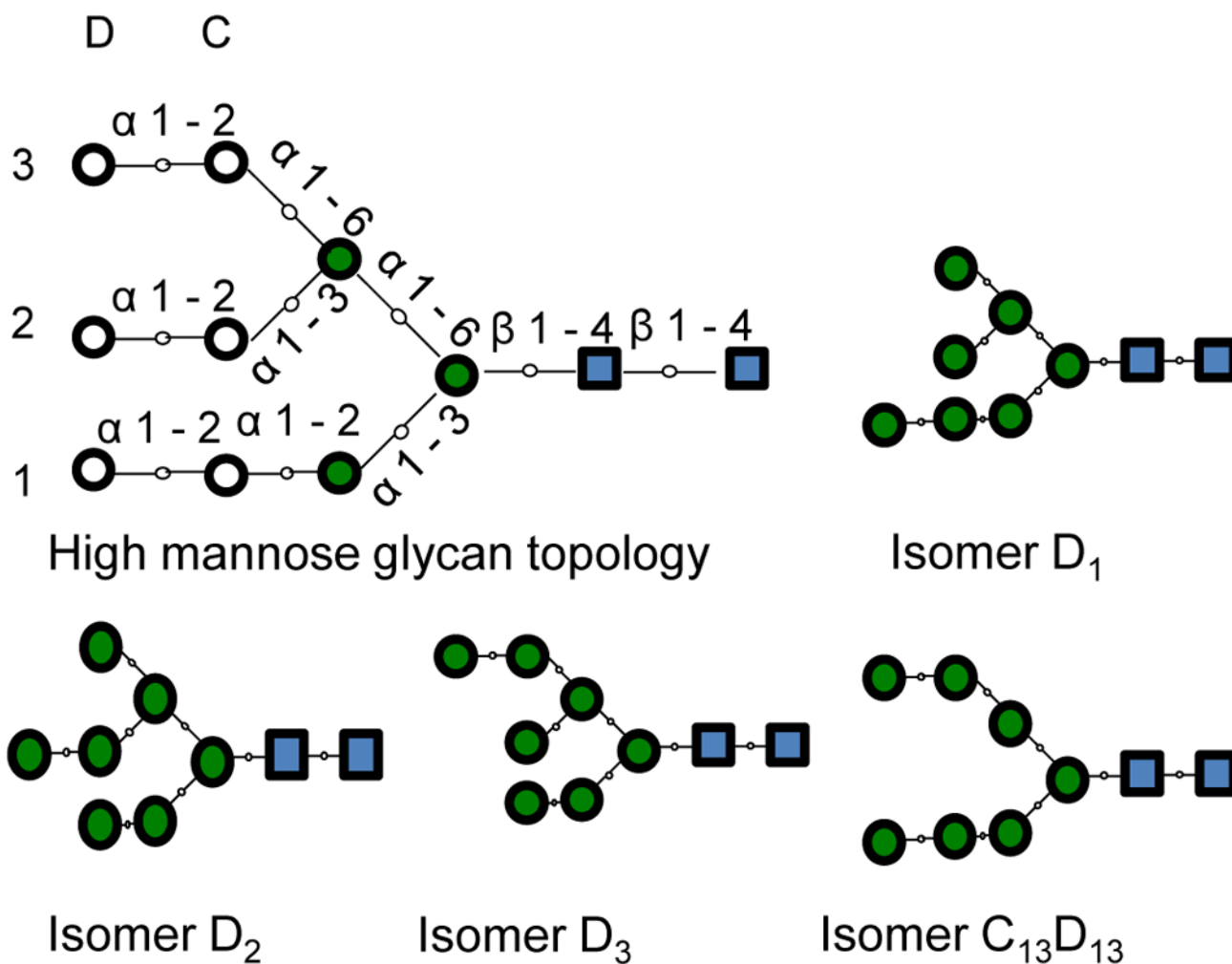
Scheme 1.

Numbering system for high-mannose glycans. The circles correspond to mannose residues. The squares indicate N-acetylglucosamine residues. The solid circles and squares compose the core of the N-glycan structure. Additional mannose residues (empty circles) can be linked to the core structure and the resulting species are named according to occupying positions (circles) of the mannose residues. For Mannose7, the D_1, D_2, and D_3 isomers refer to the structures that have the last mannose residue at D_1, D_2 and D_3 positions, respectively. The $C_{13}D_{13}$ isomer has additional mannose residues at C_1, C_3, D_1, and D_3 positions.